EXPLICIT GUIDANCE OF DRAG MODULATED AEROASSISTED TRANSFER BETWEEN ELLIPTICAL ORBITS

84-1848

Nguyen X. Vinh* and Jennie R. Johannesen**
The University of Michigan, Ann Arbor, Michigan

Kenneth D. Mease+
Jet Propulsion Laboratory, Pasadena, California

John M. Hanson†
Analytic Services, Inc., Arlington, Virginia

A84-43415

Abstract

This paper presents the complete analysis of the problem of minimum-fuel aeroassisted transfer between coplanar elliptical orbits in the case where the orientation of the final orbit is free for selection in the optimization process. The comparison between the optimal pure propulsive transfer and the idealized aeroassisted transfer, by several passages through the atmosphere, is made. In the case where aeroassisted transfer provides fuel saving, a practical scheme for its realization by one passage is proposed. The maneuver consists of three phases: A deorbit phase for non zero entry angle, followed by an atmospheric fly-through with variable drag control and completed by a post atmospheric phase. An explicit guidance formula for drag control is derived and it is shown that the required exit speed for ascent to the final orbit can be obtained with a very high degree of accuracy.

1. Introduction

The problem of minimum-fuel aeroassisted transfer between orbits has received considerable attention in recent years. The case of transfer between coplanar circular orbits has been analyzed[1-3]. In this paper, we shall consider the case where the two terminal orbits are elliptical. More specifically, it is proposed to transfer, with a minimum fuel consumption, a vehicle from an initial elliptical orbit O_1 to a coplanar final elliptical orbit O_2. The two Keplerian orbits are about a spherical planet with center of attraction located at the point F (Fig. 1). The orbits are defined by the apocenter distances A_i, and the pericenter distances P_i. We shall assume that the orientation of the line of apsides is free for selection in the optimization process. This means that the argument of the pericenter of the final orbit is not of importance in the intended mission.

For a high-thrust propulsion system, it is assumed that the time interval for powered flight is short as compared to the orbital period. Hence, we can consider the velocity changes, upon the application of the thrust, as being instantaneous.

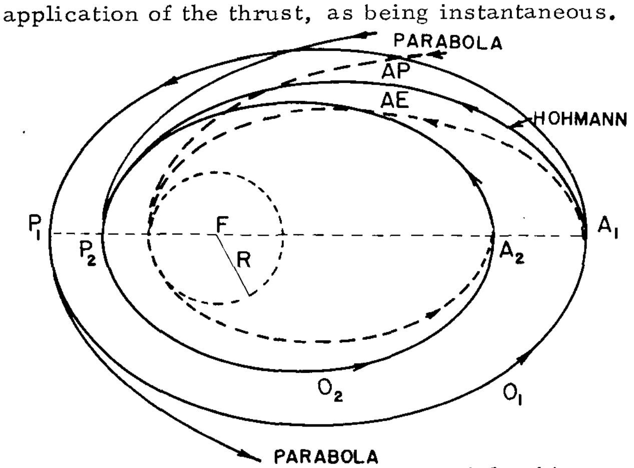

Fig. 1. Transfers between coaxial orbits.

2. Idealized Optimal Transfers

We first consider the various optimal pure propulsive transfers and select the best for comparison with the most advantageous aeroassisted transfer in an idealized scheme. This is intended to display explicitly the circumstances under which aeroassisted transfer is a fuel saving mode. In the following sections, we shall provide an analysis of its practical realization.

For a pure propulsive transfer, since the orientation of the final orbit is free, in the optimal condition the terminal orbits are coaxial with pericenters on the same side of the attracting center F[4-6]. For a finite-time transfer, the optimal mode is the Hohmann transfer connecting the higher apocenter to the pericenter of the other orbit. We shall consider the case where the apocenter of the initial orbit is higher, that is $A_1 \geq A_2$ and conveniently define the dimensionless lengths and characteristic velocities

$$\alpha_i = \frac{A_i}{R}, \quad \beta_i = \frac{P_i}{R}, \quad v = \frac{V}{\sqrt{\mu/R}}, \quad \Delta v_i = \frac{\Delta V_i}{\sqrt{\mu/R}} \tag{1}$$

where μ is the gravitational constant of the planet and R is the radius of its surrounding atmosphere. The characteristic velocity of the Hohmann transfer, normalized with respect to the circular speed at distance R, $V_c = \sqrt{gR} = \sqrt{\mu/R}$, is

* Professor of Aerospace Engineering
** Graduate student
\+ Member Technical Staff, Navigation Systems Section. Member AIAA
† Research Engineer

$$\Delta v_H = \frac{\Delta V_H}{V_c} = \left| \sqrt{\frac{2\beta_1}{\alpha_1(\alpha_1+\beta_1)}} - \sqrt{\frac{2\beta_2}{\alpha_1(\alpha_1+\beta_2)}} \right| + \sqrt{\frac{2\alpha_1}{\beta_2(\alpha_1+\beta_2)}} - \sqrt{\frac{2\alpha_2}{\beta_2(\alpha_2+\beta_2)}} \qquad (2)$$

If $\alpha_1 \to \infty$, the initial approaching orbit is parabolic and the first impulse, applied at infinity or in practice at a large distance, is negligible. This leads to conceiving a parabolic transfer, even in the case where α_1 is finite. The first accelerative impulse is applied at the pericenter of the first orbit to propel the vehicle into a parabola. At infinity, upon the application of an infinitesimal impulse, the vehicle returns by another parabola with the same pericenter as for the final orbit. Another decelerative impulse is applied at this center to complete the transfer. All the impulses are tangential and the total cost for this parabolic mode is

$$\Delta v_P = \sqrt{\frac{2}{\beta_1}} - \sqrt{\frac{2\alpha_1}{\beta_1(\alpha_1+\beta_1)}} + \sqrt{\frac{2}{\beta_2}} - \sqrt{\frac{2\alpha_2}{\beta_2(\alpha_2+\beta_2)}} \qquad (3)$$

Upon direct comparison of the characteristic velocities, one can select the optimal pure propulsive mode.

For aeroassisted transfer, a decelerative impulse is applied tangentially at the apocenter of initial orbit to lower the pericenter to the top of the atmosphere. Its magnitude is

$$\Delta v_1 = \sqrt{\frac{2\beta_1}{\alpha_1(\alpha_1+\beta_1)}} - \sqrt{\frac{2}{\alpha_1(\alpha_1+1)}} \qquad (4)$$

Near the top of the atmosphere, in the vicinity of the pericenter, atmospheric drag will work to reduce the apocenter to the distance A_2 where an accelerative impulse is applied to propel the vehicle into the final orbit. Its magnitude is

$$\Delta v_2 = \sqrt{\frac{2\beta_2}{\alpha_2(\alpha_2+\beta_2)}} - \sqrt{\frac{2}{\alpha_2(\alpha_2+1)}} \qquad (5)$$

The total cost for this aeroassisted-elliptic mode is

$$\Delta v_{AE} = \Delta v_1 + \Delta v_2 \qquad (6)$$

and it has to be compared with the best pure propulsive mode for optimality. Another way to bring the pericenter to the top of the atmosphere for the atmospheric decay process is to first send the vehicle into a parabolic orbit by a tangential and accelerative impulse applied at the pericenter of the initial orbit. Its magnitude is

$$\overline{\Delta v}_1 = \sqrt{\frac{2}{\beta_1}} - \sqrt{\frac{2\alpha_1}{\beta_1(\alpha_1+\beta_1)}} \qquad (7)$$

Then, at a large distance, we can return the vehicle for a grazing trajectory with a negligible impulse. The subsequent process of orbit decay and injection into the final orbit is as before and this time we have for this aeroassisted-parabolic mode

$$\Delta v_{AP} = \overline{\Delta v}_1 + \Delta v_2 \qquad (8)$$

By comparing the Eqs. (4) and (7), we deduce that for the two aeroassisted modes, the parabolic mode is more economical if

$$\beta_1 \geq \frac{4(\alpha_1+1)}{\alpha_1} \qquad (9)$$

The aeroassisted transfer discussed in this section is based on an idealized scheme. It will require several passages through the atmosphere for A_1 to decrease to A_2. Furthermore, based on the theory of orbit contraction, it is assumed that during the decay process, the pericenter is nearly stationary [7]. If this mode is optimal, the characteristic velocity computed is the idealized absolute minimum.

In the following sections we shall study the implementation of the aeroassisted transfer. We shall impose the constraint that the reduction of the apocenter occurs in a single passage. This requires a non-zero entry angle γ_e and exit angle γ_f. The resulting total cost will be slightly higher.

The aeroassisted transfer consists of three phases:

The first phase is the deorbit phase. A propulsive maneuver is effected such that the vehicle enters the atmosphere, at distance R, at a certain prescribed angle γ_e. This angle, which is very small, is selected such that within the drag capability of the vehicle, the necessary speed depletion can be accomplished in one passage.

The second phase is the atmospheric fly-through phase. We shall assume that the ballistic coefficient of the vehicle can be modulated between its maximum and minimum values. By a proper modulation of this coefficient, it is proposed to bring the vehicle to the best atmospheric exit condition for the vehicle to climb to the final apocenter for orbit insertion.

The third and final phase is the post atmospheric maneuver to put the vehicle into the final orbit.

It will be shown in a synthesis study that all the three phases are coupled. This means that the initial entry angle is selected based on the final orbit configuration and the drag capability of the vehicle during atmospheric passage. But, in terms of the fuel consumption, since the entry and exit angles are small, it is possible to analyze separately the optimal maneuver for each phase. It will be shown that the resulting characteristic velocity for the combined maneuver is very close to the idealized minimum.

3. Entry at Prescribed Angle

In the deorbit phase, it is proposed to find the optimal descending trajectory which intersects the atmosphere, at distance R at a non-zero prescribed angle γ_e. This can be achieved by applying a single, tangential and decelerative impulse at the apocenter of the initial orbit. From the geometry of the deorbit as shown in Fig. 2, the characteristic velocity for this one-impulse mode is

$$\Delta v_I = \sqrt{\frac{2\beta_1}{\alpha_1(\alpha_1+\beta_1)}} - \sqrt{\frac{2(\alpha_1-1)}{\alpha_1(\alpha_1^2-\cos^2\gamma_e)}}\cos\gamma_e \tag{10}$$

The cost for deorbit increases as the entry angle increases.

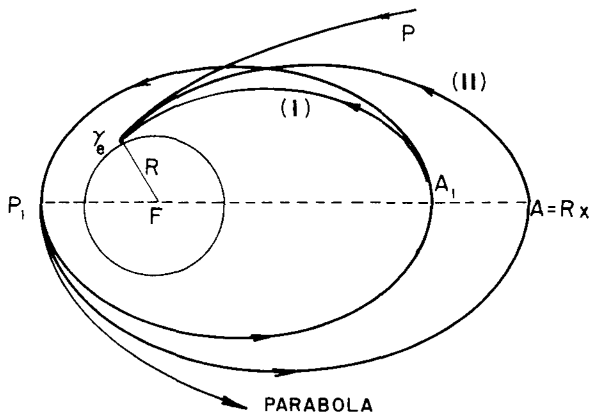

Fig. 2. Deorbit for prescribed entry angle.

Another alternative is to use parabolic orbits for deorbiting. In this case, an accelerative impulse is applied tangentially at the pericenter to send the vehicle into a parabola. Then at infinity, we can return the vehicle along another parabola for entry at any prescribed angle with an infinitesimal impulse. The cost for this transfer is given in Eq. (7). By comparing this equation with Eq. (10) we have the explicit condition for the parabolic mode to be better than the one-impulse mode.

$$\beta_1 \geq \frac{4(\alpha_1-1)(\alpha_1^2-\cos^2\gamma_e)\cos^2\gamma_e}{\alpha_1(\alpha_1-\cos^2\gamma_e)^2} \tag{11}$$

The simple criterion (11) is used to rule out either the one-impulse mode or the parabolic mode. But for non-zero entry angle, there exists the possibility of the two-impulse mode as the optimal process. In this case, the first and accelerative impulse is applied tangentially at the pericenter of the initial orbit to bring the apocenter to the distance $A = R\,x$. The characteristic velocity for this maneuver is

$$\Delta v_1 = \sqrt{\frac{2x}{\beta_1(x+\beta_1)}} - \sqrt{\frac{2\alpha_1}{\beta_1(\alpha_1+\beta_1)}} \tag{12}$$

At the new apocenter, a second tangential and decelerative impulse is applied to return the vehicle for intersection at the prescribed angle. Its magnitude is

$$\Delta v_2 = \sqrt{\frac{2\beta_1}{x(x+\beta_1)}} - \sqrt{\frac{2(x-1)}{x(x^2-\cos^2\gamma_e)}}\cos\gamma_e \tag{13}$$

The total characteristic velocity for this two-impulse deorbit is

$$\Delta v_{II} = \Delta v_1 + \Delta v_2 \tag{14}$$

For given elements (α_1, β_1) of the initial orbit and entry angle γ_e, this is a function of the out going distance x. By minimizing the function with respect to x, we are led to the necessary condition

$$\sqrt{\frac{\beta_1(x-1)(x^2-\cos^2\gamma_e)^3}{(x+\beta_1)\cos^2\gamma_e}} = 2x^3 - 3x^2 + \cos^2\gamma_e \tag{15}$$

Upon solving for x and using its value in Eqs. (12)-(14), we have the minimum characteristic velocity for the two-impulse mode.

We observe that, the one-impulse mode, when it becomes optimal, can be viewed as the limiting case of the two-impulse mode when $x = \alpha_1$. Hence, using this limit in Eq. (15), we have the condition for the two-impulse mode to be more economical than the one-impulse mode.

$$\sqrt{\frac{\beta_1(\alpha_1-1)(\alpha_1^2-\cos^2\gamma_e)^3}{(\alpha_1+\beta_1)\cos^2\gamma_e}} \geq 2\alpha_1^2(\alpha_1-1) - (\alpha_1^2-\cos^2\gamma_e) \tag{16}$$

In summary, the optimal mode depends on the parameters α_1, β_1 and γ_e. For a practical application, we first check condition (16). If the one impulse mode is better, then condition (11) can be used to decide the optimal mode. If the two-impulse mode is better, and if condition (11) is not satisfied, then the optimal mode is obviously the two-impulse mode.

As an example, we consider the case where the initial orbit is circular with radius r_1 and summarize the results in Fig. 3.

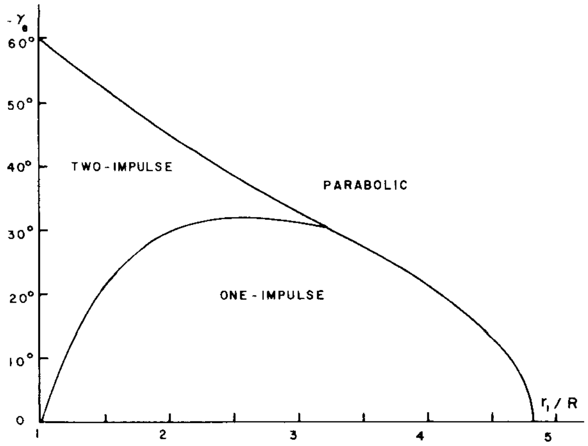

Fig. 3. Regions of optimality for deorbit from circular orbit with prescribed entry angle.

4. Explicit Guidance for Drag Modulation

We consider in this section the atmospheric phase in the aeroassisted maneuver. To begin this phase, the vehicle enters the atmosphere, at distance R with a speed V_e and entry angle γ_e. The atmospheric maneuver consists of using lift or drag modulation to bring the vehicle to exit at $\gamma_f \approx 0$ and with a resulting exit speed V_f such that the apocenter of the ascending trajectory coincides with the apocenter of the final orbit (Fig. 4). In this way, the final impulse is minimized.

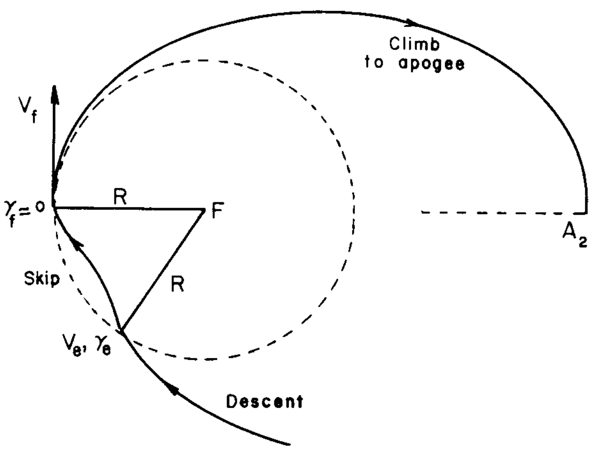

Fig. 4. Aeroassisted transfer.

We shall consider the case where it is possible to modulate the ballistic drag coefficient between a lower and an upper limit. Using standard notation, we have the equations for ballistic flight inside a non-rotating planetary atmosphere.

$$\frac{dr}{dt} = V \sin\gamma$$

$$\frac{dV}{dt} = -\frac{\rho S C_D V^2}{2m} - g \sin\gamma \qquad (17)$$

$$V\frac{d\gamma}{dt} = \left(\frac{V^2}{r} - g\right)\cos\gamma \qquad (17)$$

Since the flight path angle stays small, (a few degrees),we can neglect the small gravity component g sin γ as compared to the acceleration due to the drag. Furthermore, we use the approximations

$$\sin\gamma \approx \gamma,\ \cos\gamma \approx 1,\ g(r) \approx g(R),\ \frac{V^2}{r} \approx \frac{V^2}{R} \qquad (18)$$

These approximations induce an error of the same order as the error committed by neglecting the Coriolis force. It should be mentioned that the assumptions used are not necessary for the present analysis but they have the advantage of displaying explicitly the various effects of drag coefficient, entry speed and entry angle on the ballistic fly-through trajectory[8].

We shall use the density ρ as the altitude variable and assume that this density is locally exponential, that is

$$\frac{d\rho}{\rho} = -\frac{dr}{H} \qquad (19)$$

where the scale height H can be adjusted for concordance with the standard atmosphere at the altitude range of the flight. Then, with the simplification (18) and by using the dimensionless variables

$$y = \frac{\rho}{\rho_e},\quad \Phi = -\sqrt{\frac{R}{H}}\,\gamma,\quad x = \log\left(\frac{V_e}{V}\right)^2,\quad \theta = \sqrt{\frac{g}{H}}\,t \qquad (20)$$

and the parameters

$$\delta = \frac{gR}{V_e^2},\quad \epsilon = \frac{\rho_e S C_D \sqrt{HR}}{m} \qquad (21)$$

we have the equations of motion in dimensionless form

$$\frac{dy}{dx} = \frac{\Phi}{\epsilon}$$

$$\frac{d\Phi}{dx} = \frac{(\delta e^x - 1)}{\epsilon y} \qquad (22)$$

and

$$\frac{d\theta}{dx} = \frac{\sqrt{\delta}\, e^{x/2}}{\epsilon y} \qquad (23)$$

We notice that the last equation denoting the variation of the time is decoupled. The constant δ represents the effect of the entry speed with $\delta = 1$ for circular entry and $\delta = 0.5$ for parabolic entry. The parameter ϵ is the drag control parameter, subject to the constraint

$$\epsilon_{min} \leq \epsilon \leq \epsilon_{max} \qquad (24)$$

In this way, the design of drag control is more flexible since it is not restricted to the variation of the drag coefficient C_D alone. We simply assume that the dimensionless drag parameter ϵ, as defined in Eq. (21) can be configured to vary between two limits. The speed variable x is such that, at the initial time, $x = 0$ and it is monotonically increasing, that is, larger x for lower current speed. The altitude y is such that initially $y = 1$ and it increases as the altitude decreases. At exit, we have $y_f = y_e = 1$. In the definition of the flight path angle variable Φ, the ratio R/H can be taken as 900 for the Earth's atmosphere.

From the definition (20) of the dimensionless variables, we have at the initial time

$$\theta = 0, \quad x = 0, \quad y_e = 1, \quad \Phi_e = -\sqrt{R/H}\ \gamma_e = c > 0 \tag{25}$$

It is proposed to use the drag control ϵ, subject to the constraint (24), to bring the vehicle to exit at

$$x = x_f, \quad y_f = 1, \quad \Phi_f = -\sqrt{R/H}\ \gamma_f \tag{26}$$

such that

1. The apocenter distance of the ascending orbit is A_2.
2. The speed at this center is maximized.

The first condition is expressed as the constraint

$$v_f^2(\alpha_2^2 - \cos^2\gamma_f) = 2\alpha_2(\alpha_2 - 1) \tag{27}$$

where in terms of the speed variable x, we have

$$v_f^2 = \frac{1}{\delta} e^{-x_f} \tag{28}$$

The second condition leads to the maximization of the performance index

$$J = v_a^2 = v_f^2 + \frac{2}{\alpha_2} - 2 = \frac{2(\alpha_2 - 1)\cos^2\gamma_f}{\alpha_2(\alpha_2^2 - \cos^2\gamma_f)} \tag{29}$$

Since $\alpha_2 = A_2/R$ is prescribed, this amounts to maximizing the final exit speed satisfying the condition (27). From this condition, we see that the best exit speed is obtained when $\gamma_f = 0$, if this can be achieved. The resulting maximized exit speed is

$$v_f = \sqrt{\frac{2\alpha_2}{\alpha_2 + 1}} \tag{30}$$

For a drag modulation, grazing exit for a climb to apocenter is not possible[8], and the optimal strategy consists of bang-bang control to achieve condition (27) with the smallest exit angle[1]. This control strategy is difficult to realize in practice since the switching time θ_s has to be very accurate, to within a fraction of one second to avoid crashing.

As an alternative, we propose the following drag control. First, a nominal trajectory is selected, with entry condition γ_e and v_e, such that during the atmospheric phase with a high drag coefficient $\epsilon = \epsilon_1$ for descent until $\gamma = 0$, and a low drag coefficient $\epsilon = \epsilon_2$ for ascent until exit, we have a shallow exit angle and the trajectory overshoots the target apocenter. On the other hand, γ_e and v_e are selected such that a trajectory with a constant high drag coefficient $\epsilon = \epsilon_1$ undershoots the target apocenter. The nominal drag coefficients ϵ_1 and ϵ_2 are selected to be consistent with the physical constraint $\epsilon_{max} \geq \epsilon_1 > \epsilon_2 \geq \epsilon_{min}$. These conditions ensure that in the actual trajectory, by using a modulated drag coefficient, ϵ = variable, during the ascending phase we can achieve the required apocenter distance while obtaining a small exit angle.

Since it is difficult to control both γ_f and v_f to satisfy Eq. (27) identically, our proposed explicit guidance scheme aims at controlling v_f. The reason for this is that, based on Eq. (27) for a sensitivity analysis, we have for small exit angle

$$\frac{\Delta\alpha_2}{\alpha_2} = \frac{v_f^2}{(\alpha_2 - v_f^2)}\left[(\alpha_2^2 - 1)\left(\frac{\Delta v_f}{v_f}\right) + \gamma_f^2\left(\frac{\Delta\gamma_f}{\gamma_f}\right)\right] \tag{31}$$

The variation in the apocenter is more sensitive to the exit speed perturbation than to the exit angle perturbation.

To develop a variable drag control law, we consider a nominal skip trajectory as shown in Fig. 5. This trajectory, flown with $\epsilon = \epsilon_1$ until the bottom of the flight path, $\gamma_b = 0$, and $\epsilon = \epsilon_2$ until exit, provides an exit speed v_f^o and a flight path angle γ_f^o. As mentioned above, this trajectory is designed to overshoot the terminal apocenter A_2. To have a correct distance α_2, we can use a higher variable drag coefficient ϵ during the ascent for an exit at v_f and γ_f satisfying the constraint (27).

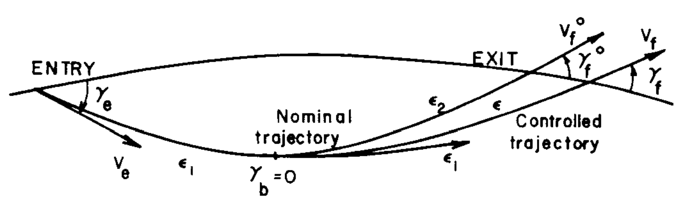

Fig. 5. Nominal trajectory and controlled trajectory.

We then select a value $\gamma_f < \gamma_f^o$ and compute the desired speed v_f from Eq. (27). The objective is to obtain a formula for a variable ϵ such that at exit we have a resulting speed $\overline{v}_f = v_f$, with an exit angle $\overline{\gamma}_f$ relatively close to the correct value γ_f. In terms of the variables x and Φ, we use the definition (20). Based on the first of the equations (22), during the ascent, from any current position, we can predict the exit speed, in the case where ϵ is held constant for the remainder of the trajectory, by integrating the equation until $y_f = 1$. An analytic solution is possible if we use an average value Φ_a for the flight path angle variable. We have

$$y - 1 = - \frac{\Phi_a (x_f - x)}{\epsilon} \tag{32}$$

For the average value Φ_a, we can use the mean value between the current value Φ and the estimated exit value Φ_f. This leads us to use the control law

$$\epsilon = - \frac{(\Phi + \Phi_f)(x_f - x)}{2(y - 1)} \tag{33}$$

where x_f is the desired final speed and Φ_f is the estimated exit flight path angle variable. This control law is explicit since ϵ is continuously recomputed based on the current state, rather than on the deviation of the current state from a nominal current state. It remains to evaluate the estimated exit angle Φ_f. By combining the two equations (22), we have

$$\frac{dy}{y} = \frac{\Phi \, d\Phi}{(\delta e^x - 1)} \tag{34}$$

By keeping $(\delta e^x - 1)$ constant, we neglect the effect of the variation of the speed. This is a good assumption since most of the speed depletion occurs during the descending phase at high drag coefficient. By integrating Eq. (34) from the lowest point, $y = y_b$, $\Phi = 0$, to exit $y = 1$, $x = x_f$, we have the estimated value for Φ_f

$$\Phi_f^2 = 2(1 - \delta e^{x_f}) \log y_b + k \tag{35}$$

In this equation, we have introduced an additive correctional term k to compensate for the error incurred in neglecting the effect of the variation of the speed. This value k is computed based on the nominal trajectory by using in Eq. (35) $\Phi_f = \Phi_f^o$, $x_f = x_f^o$. The key to the efficacy of this approach is that, for the family of skip trajectories under consideration, the flight path angle behavior is relatively uniform: the flight path angle is always small (a few degrees at most); and it is monotonically increasing during the guided portion of the flight which starts at $\gamma = \gamma_b = 0$. Consequently, the flight path angle is of minor importance in comparison with the speed. The connection of the guidance law with the nominal trajectory, since it is embodied in the constant k which only affects the flight path angle, is minimal and does little to disrupt the explicit nature of the guidance law.

This explicit drag modulated control law has been tested numerically for several values of the entry speed ranging from parabolic entry, $\delta = 0.5$, to near circular entry, $\delta = 0.9$, with excellent results. The characteristic values for the ballistic drag coefficient selected are

$$\begin{aligned} \epsilon_{max} &= 0.0030 \\ \epsilon_1 &= 0.0025 \\ \epsilon_2 &= 0.0005 \\ \epsilon_{min} &= 0.0002 \end{aligned} \tag{36}$$

We can of course use the values ϵ_1 and ϵ_2 at ϵ_{max} and ϵ_{min} respectively in constructing the nominal trajectory. The main effect of the ratio $\epsilon_{max}/\epsilon_{min}$ is in the widening of the family of trajectories which can be accurately controlled. The numerical results are summarized in Tables 1 and 2.

In Table 1, we have the case of parabolic entry, $\delta = 0.5$, $v_e = \sqrt{2}$, $\gamma_e = -3.82^o$. The drag sequence $\epsilon_1 \rightarrow \epsilon_2$ with switching at the bottom of the trajectory leads to $x_f^o = 0.394717$, $\gamma_f^o = 2.8307^o$. We also have $y_b = 63.7253$ with the correctional term $k = 0.05284865$. In the table, x_f is the required exit speed while $\overline{x}_f$ is the actual resulting exit speed with the variable drag control law (33). We can see in the table that the speed control is excellent, not only near the nominal trajectory, but for a large range from high speed exit to low speed exit. The value γ_f is the one computed from Eq. (35). Using x_f and γ_f, we have computed α_2 from Eq. (27). Hence, using this table, we consider the problem as of controlling the vehicle for exit at x_f, γ_f for an ascent to α_2. The actual results are $\overline{x}_f$, $\overline{\gamma}_f$ and $\overline{\alpha}_2$.

In Table 2, we have the case of $\delta = 0.577$, $v_e = 1.316473$, $\gamma_e = -3.36^o$. This is essentially the entry speed for a direct return from a geosynchronous orbit. The relevant data from the nominal trajectory, $\epsilon_1 \rightarrow \epsilon_2$, are $x_f^o = 0.307536$, $\gamma_f^o = 2.4787^o$, $y_b = 45.4944$ and $k = 0.04101062$.

Other cases of lower entry speed were tested with excellent results and it can be concluded that this explicit variable drag controls accurately the exit speed.

The variations of the drag coefficient ϵ during the controlled ascent are shown in Fig. 6 for the case of a return from a geosynchronous orbit. Typically, because we control the skip trajectory for an exit speed lower than the nominal exit speed, that is for $x_f > x_f^o$, the modulated flight for ascent starts at y_b with an initial drag coefficient $\epsilon > \epsilon_2$. For high speed exit, ϵ decreases continuously until exit, $y_f = 1$. For low speed exit, ϵ increases to provide more speed depletion. It should be mentioned that, by using variable drag coefficient during ascent, the sensitivity problem encountered in bang-bang control is removed. Here, the switching time is no longer a critical

Table 1. Accuracy analysis for adaptive drag modulation mode
Case of parabolic entry, $\delta = 0.5$

x_f	$\bar{x}_f$	$V_f/\bar{V}_f$	γ_f(deg.)	$\bar{\gamma}_f$(deg.)	$\Delta\gamma_f$(deg.)	α_2	$\bar{\alpha}_2$	$\Delta\alpha_2$
0.400	0.400000	1.000000	2.809575	2.798629	-0.010946	2.037951	2.037915	-0.000036
0.425	0.425000	1.000000	2.705810	2.703902	-0.001908	1.892964	1.892958	-0.000006
0.450	0.450000	1.000000	2.595113	2.604145	0.009032	1.764316	1.764349	0.000033
0.475	0.475000	1.000000	2,476482	2.498979	0.022497	1.649427	1.649512	0.000085
0.500	0.500000	1.000000	2.348635	2.388049	0.039414	1.546233	1.546392	0.000159
0.525	0.525000	1.000000	2.209885	2.271085	0.061200	1.453065	1.453329	0.000264
0.550	0.550000	1.000000	2.057932	2.148060	0.090128	1.368557	1.368978	0.000421
0.575	0.575000	1.000000	1.889486	2.019531	0.130045	1.291583	1.292253	0.000670
0.600	0.600000	1.000000	1.699530	1.887452	0.187922	1.221206	1.222305	0.001099
0.625	0.624998	0.999999	1.479658	1.757248	0.277590	1.156650	1.158582	0.001932
0.650	0.649357	0.999679	1.213539	1.644051	0.430512	1.097286	1.102504	0.005218

Table 2. Accuracy analysis for adaptive drag modulation mode
Case of direct return from geosynchronous orbit, $\delta = 0.577$

x_f	$\bar{x}_f$	$V_f/\bar{V}_f$	γ_f(deg.)	$\bar{\gamma}_f$(deg.)	$\Delta\gamma_f$(deg.)	α_2	$\bar{\alpha}_2$	$\Delta\alpha_2$
0.325	0.325000	1.000000	2.399299	2.398029	-0.001270	1.678884	1.678880	-0.000004
0.350	0.350000	1.000000	2.279466	2.290667	0.011201	1.572704	1.572746	0.000042
0.375	0.375000	1.000000	2.149113	2.176852	0.027739	1.476966	1.477077	0.000111
0.400	0.400000	1.000000	2.006688	2.056302	0.049614	1.390230	1.390445	0.000215
0.425	0.425000	1.000000	1.849303	1.928839	0.079536	1.311310	1.311688	0.000378
0.450	0.450000	1.000000	1.672627	1.795253	0.122626	1.239221	1.239876	0.000655
0.475	0.475000	1.000000	1.469588	1.658553	0.188965	1.173144	1.174321	0.001177
0.500	0.499955	0.999978	1.227008	1.528180	0.301172	1.112400	1.114747	0.002347
0.525	0.519449	0.997228	0.913699	1.444393	0.530694	1.056492	1.062457	0.005965

parameter in the process. By using the control law (33), even in the case where it is not started exactly at the lowest point, it is self-corrective by using the current state to adjust the drag and, as a consequence, leads to the desired exit speed.

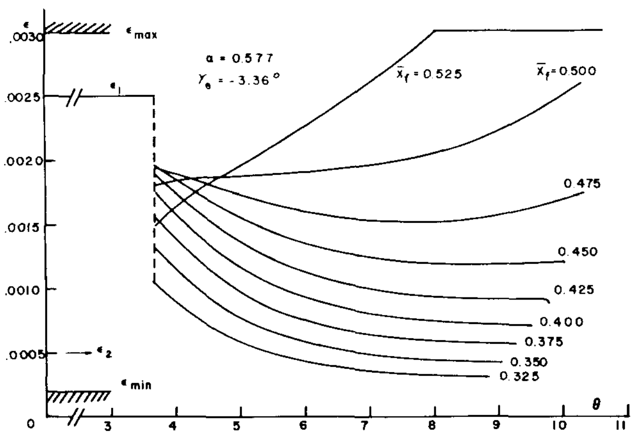

Fig. 6. Variations of the drag coefficient ϵ for various exit speeds in the case of a return from a geosynchronous orbit.

5. Optimal Post Atmospheric Maneuver

We have seen in the previous section that at exit we have $\bar{v}_f$, $\bar{\gamma}_f$ leading to an apocenter distance $\bar{\alpha}_2$. If $\bar{\alpha}_2 = \alpha_2$, a final impulse, applied tangentially at this apocenter distance, is necessary for optimal orbit insertion. We consider the general case where $\bar{\alpha}_2 \neq \alpha_2$ and optimize this post atmospheric phase.

The case where we overshoot the target apocenter, $\bar{\alpha}_2 > \alpha_2$, is simple. The final orbit is achieved by a Hohmann transfer with an accelerative impulse at $\bar{\alpha}_2$ to raise the pericenter to the level β_2 and a decelerative impulse at this center to adjust $\bar{\alpha}_2$ to the correct distance α_2.

In the case where we undershoot the target apocenter, $\bar{\alpha}_2 < \alpha_2$, the first impulse Δv_1 is applied at the lowest point which is the exit point, to bring $\bar{\alpha}_2$ to α_2. At this correct apocenter, a tangential and accelerative impulse Δv_2 is applied for orbit insertion. The velocity diagram at exit is shown in Fig. 7 with the Y-axis along the position vector.

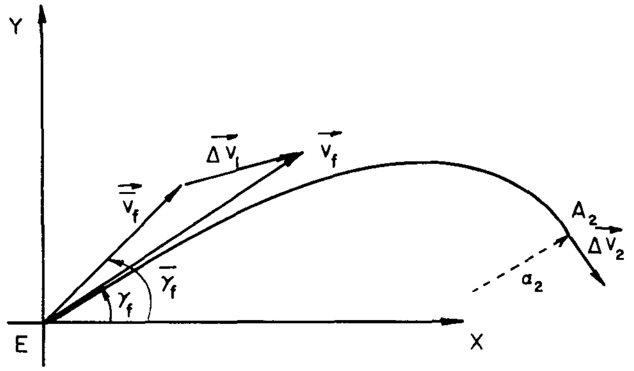

Fig. 7. Velocity diagram at exit.

In this system we have the components

$$\bar{X} = \bar{v}_f \cos \bar{\gamma}_f \ , \quad \bar{Y} = \bar{v}_f \sin \bar{\gamma}_f \tag{37}$$

of the exit velocity $\vec{\bar{v}}$ resulting from drag modulated fly through and the components

$$X = v_f \cos \gamma_f \ , \quad Y = v_f \sin \gamma_f \tag{38}$$

of the correct velocity $\vec{v}_f$ required for attaining the final apocenter distance α_2. Expressed in terms of X and Y, we write the constraining relation (27)

$$(\alpha_2^2 - 1) X^2 + \alpha_2^2 Y^2 - 2\alpha_2(\alpha_2 - 1) = 0 \tag{39}$$

Let v_2 be the speed at the apocenter in the final orbit. The sum of the two impulses Δv_1 and Δv_2 required in post atmospheric maneuver is

$$J = \sqrt{(X - \bar{X})^2 + (Y - \bar{Y})^2} + v_2 - \frac{X}{\alpha_2} \tag{40}$$

Taking account of the constraint (39) we introduce the Lagrange multiplier λ and minimize the augmented function

$$I = J + \lambda [(\alpha_2^2 - 1) X^2 + \alpha_2^2 Y^2 - 2\alpha_2 (\alpha_2 - 1)] \tag{41}$$

The necessary conditions for a stationary value of I are

$$\frac{\partial I}{\partial X} = 0 \ , \quad \frac{\partial I}{\partial Y} = 0 \tag{42}$$

Upon eliminating λ between these equations and simplifying the result, we obtain

$$Y - \bar{Y} = k_1 (\bar{Y} X - \bar{X} Y) \tag{43}$$

where

$$k_1 = \sqrt{\frac{\alpha_2(\alpha_2 + 1)}{2}} \tag{44}$$

Define the components of the first impulse which is non tangential

$$\begin{aligned} \Delta X &= X - \bar{X} \\ \Delta Y &= Y - \bar{Y} \end{aligned} \tag{45}$$

From the linear equation (43), we deduce the optimal thrust angle

$$\tan \psi = \frac{\Delta Y}{\Delta X} = \frac{k_1 \bar{Y}}{1 + k_1 \bar{X}} \tag{46}$$

which can be immediately evaluated for given α_2, $\bar{v}_f$ and $\bar{\gamma}_f$.

Let

$$k_2 = \frac{\bar{Y}}{1 + k_1 \bar{X}} \tag{47}$$

and write Eq. (43) as

$$Y = k_2 (1 + k_1 X) \tag{48}$$

Upon substituting into Eq. (39) and solving for the positive root, we obtain the solution

$$\begin{aligned} X &= \frac{k_1 [2(\alpha_2 - 1) \sqrt{1 + k_1^2 k_2^2} - \alpha_2^2 k_2^2]}{(\alpha_2^2 - 1) + \alpha_2^2 k_1^2 k_2^2} \\ Y &= \frac{(\alpha_2^2 - 1) k_2 [1 + \alpha_2 \sqrt{1 + k_1^2 k_2^2}]}{(\alpha_2^2 - 1) + \alpha_2^2 k_1^2 k_2^2} \end{aligned} \tag{49}$$

With this solution the minimum characteristic velocity in post atmospheric flight is

$$\Delta v_1 + \Delta v_2 = v_2 + \sqrt{\frac{2\alpha_2}{\alpha_2 + 1}} - \sqrt{\bar{Y}^2 + \frac{(1 + k_1 \bar{X})^2}{k_1^2}} \tag{50}$$

Hence, just as for the thrust angle, the minimum cost can be evaluated immediately in terms of α_2, $\bar{v}_f$ and $\bar{\gamma}_f$ without having to go through intermediary steps. An elegant geometric solution based on hodograph theory has been given by Marchal[9].

6. Problem Synthesis

From the previous analysis, it is clear that for aeroassisted transfer, the three phases involved are coupled in terms of the total fuel consumption. The final apocenter distance and the drag capability dictate the selection of the entry elements γ_e and v_e which in turn influence the characteristic velocity for the deorbit phase. In this section, we shall prove the assertion that, as compared to the idealized case, which is not realistic in practice, the penalty in the fuel consumption using the present operating mode is small since the optimal condition has been realized in each phase.

We first compute the additional fuel consumption, in terms of the characteristic velocity, $\delta(\Delta v)$, for a non zero entry angle γ_e, as compared to the idealized grazing entry case.

If parabolic deorbit is optimal, then γ_e has no influence and trivially $\delta(\Delta v) = 0$. For a finite-time deorbit, then when $\gamma_e = 0$, the optimal mode is always by one impulse. For $\gamma_e \neq 0$, there is a possibility of a two-impulse optimal mode, but even if it is the case, since γ_e is small, the saving in the fuel consumption is small. Therefore, we compare the one impulse mode which can be optimal or non optimal for non zero γ_e, with the optimal one impulse for the idealized case where $\gamma_e = 0$. By comparing Eqs. (4) and (10) and linearizing for small γ_e, we have the additional characteristic velocity

$$\delta(\Delta v) = \frac{\alpha_1^2 \gamma_e^2}{2(\alpha_1^2 - 1)} \sqrt{\frac{2}{\alpha_1(\alpha_1+1)}} = K(\alpha_1)\,\gamma_e^2 \quad (51)$$

The factor $K(\alpha_1)$ is a function of the apocenter distance of the initial orbit. It is large only for $\alpha_1 \approx 1$. But, this is not the case since aero-assisted transfer is only relevant for high initial orbit. Hence, this additional characteristic velocity is small since it is of the order of γ_e^2.

The additional fuel consumption for post atmospheric maneuver is due to non-zero exit angle. As has been mentioned above, this cannot be avoided due to the fact that for one-passage drag control, supercircular speed exit at zero exit angle is not possible. We first evaluate $\delta(\Delta v)$ for the undershoot case. For the idealized case, we have a single impulse applied at the correct apocenter with magnitude

$$\Delta v_I = v_2 - \sqrt{\frac{2}{\alpha_2(\alpha_2+1)}} \quad (52)$$

On the other hand, the minimum total characteristic velocity in post atmospheric flight for the undershoot case has been given in Eq. (50). Taking the difference, we have

$$\delta(\Delta v) = \sqrt{\frac{2(\alpha_2+1)}{\alpha_2}} - \frac{1}{k_1}\sqrt{k_1^2 \bar{v}_f^2 + 2k_1 \bar{v}_f \cos\bar{\gamma}_f + 1} \quad (53)$$

where k_1 is defined in Eq. (44) and $\bar{v}_f$ and $\bar{\gamma}_f$ are the actual exit speed and flight path angle resulting from the controlled atmospheric flight.

We recall that, in atmospheric flight, we select a small value γ_f and control the drag to have an exit speed satisfying Eq. (27). To the order of γ_f^2, we have

$$v_f^2 = \frac{2\alpha_2(\alpha_2 - 1)}{(\alpha_2^2 - \cos^2\gamma_f)} = \frac{2\alpha_2}{\alpha_2+1}\left[1 - \frac{\gamma_f^2}{(\alpha_2^2 - 1)}\right] \quad (54)$$

We have shown that we can accurately control this speed. Hence in Eq. (53), we can take $\bar{v}_f = v_f$ and compute

$$k_1^2 v_f^2 + 2k_1 v_f \cos\bar{\gamma}_f + 1 = (\alpha_2+1)^2 - \frac{\alpha_2 \gamma_f^2}{\alpha_2 - 1} - \alpha_2 \bar{\gamma}_f^2$$

Since in the undershoot case $\bar{\gamma}_f < \gamma_f$, in the last equation, by taking $\bar{\gamma}_f = \gamma_f$, we have a conservative estimate of $\delta(\Delta v)$. Then, upon substituting into Eq. (53), we have

$$\delta(\Delta v) = \frac{\alpha_2^2 \gamma_f^2}{2(\alpha_2^2 - 1)} \sqrt{\frac{2}{\alpha_2(\alpha_2+1)}} = K(\alpha_2)\,\gamma_f^2 \quad (55)$$

This has the same functional form as Eq. (51). Although here we have the case of small value of α_2, but when $\alpha_2 \approx 1$, γ_f is generally very small. For example, for an Earth orbit, taking the entry altitude at 120 km and for a very low final apocenter at 380 km, we have R = 6498 km, A_2 = 6758 km, and $\alpha_2 = 1.04$ and the function K has the value $K(\alpha_2) = 6.4347$ and is still acceptable for low exit angle.

For the overshoot case, we first compute the miss distance $\Delta\alpha_2 = \bar{\alpha}_2 - \alpha_2 > 0$. From Eq. (31), with accurate control in the speed, $\Delta v_f = 0$, and with the aid of Eq. (54) for v_f^2, we have

$$\frac{\Delta\alpha_2}{\alpha_2} = \frac{2}{(\alpha_2 - 1)}\gamma_f \Delta\gamma_f \quad (56)$$

This simple formula provides results in excellent agreement with the data in Tables 1 and 2.

For the overshoot case, post atmospheric maneuver is the usual Hohmann transfer using two impulses. Let $\bar{v}_a$ be the speed of the vehicle at the overshoot apocenter distance $\bar{\alpha}_2$. The characteristic velocity for the Hohmann transfer is

$$\Delta v_{II} = \sqrt{\frac{2\beta_2}{\bar{\alpha}_2(\bar{\alpha}_2+\beta_2)}} - \bar{v}_a + \sqrt{\frac{2\bar{\alpha}_2}{\beta_2(\bar{\alpha}_2+\beta_2)}} - \sqrt{\frac{2\alpha_2}{\beta_2(\alpha_2+\beta_2)}} \quad (57)$$

Linearizing with respect to $\Delta\alpha_2$, we have

$$\Delta v_{II} = v_2\left[1 - \frac{\Delta\alpha_2}{2\alpha_2}\right] - \bar{v}_a \quad (58)$$

where

$$v_2 = \sqrt{\frac{2\beta_2}{\alpha_2(\alpha_2+\beta_2)}} \quad (59)$$

is the speed at the apocenter on the final orbit. By comparing Eq. (58) with the idealized cost (52), we have the additional fuel consumption

$$\delta(\Delta v) = \sqrt{\frac{2}{\alpha_2(\alpha_2+1)}} - \bar{v}_a - \frac{v_2 \Delta \alpha_2}{2\alpha_2} \tag{60}$$

Using Eq. (29) to evaluate $\bar{v}_a$, with $\alpha_2 = \bar{\alpha}_2$ and v_f^2 from Eq. (54), we have

$$\bar{v}_a = \sqrt{\frac{2}{\alpha_2(\alpha_2+1)}} \left[1 - \frac{\alpha_2^2}{2(\alpha_2^2-1)} \gamma_f^2 - \frac{(\alpha_2+1)}{2\alpha_2} \Delta\alpha_2\right] \tag{61}$$

Then, upon substituting into Eq. (60) and using Eq. (56) for $\Delta\alpha_2/\alpha_2$, we have the final expression

$$\delta(\Delta v) = K(\alpha_2)\gamma_f^2 + \frac{\gamma_f \Delta\gamma_f}{(\alpha_2-1)}\sqrt{\frac{2}{\alpha_2}}\left[\sqrt{\alpha_2+1} - \sqrt{\frac{\beta_2}{\alpha_2+\beta_2}}\right] \tag{62}$$

Since $K(\alpha_2)$ is the same as in Eq. (55), and the product $\gamma_f \Delta\gamma_f$ is very small, the penalty in the characteristic velocity for the overshoot case is the same as for the undershoot case.

To conclude this paper one final remark is in order. By inspection of Tables 1 and 2 one can observe that the control in the exit flight path angle is poorer for very low values of α_2. This is of no real consequence since in practice one would not choose the particular nominal reference trajectory to control low values of α_2. For example, recall that for Table 2 (entry from geosynchronous orbit) the nominal trajectory had an entry flight path angle $\gamma_e = -3.36^o$, leading to an exit at $\gamma_f^o = 2.4787^o$ for a speed of $v_f^o = 1.128838$ and giving a nominal apocenter distance of $\alpha_2^o = 1.760183$. According to the formulation of the guidance algorithm this nominal trajectory is used to control the orbits with α_2 slightly below this value. For low altitude final orbits, the nominal trajectory selected in practice would have a steeper entry angle than $\gamma_e = -3.36^o$ which then would yield a lower nominal apocenter distance. The control algorithm would then provide excellent accuracy in the exit flight angle as well as the exit speed. For values of α_2 higher than those shown in Table 2, one would select a nominal trajectory with a more shallow entry flight path angle so as to give a higher nominal apocenter distance.

Acknowledgement. This work was supported by the Jet Propulsion Laboratory under contract No. 956416. The authors thank F. A. McCreary of JPL for her support in obtaining some of the numerical results.

References

1. Kechichian, J. A., M. I. Cruz, N. X. Vinh, and E. A. Rinderle, "Optimization and Closed Loop Guidance of Drag-Modulated Aeroassisted Orbital Transfer." AIAA paper No. 83-2093, AIAA 10th Atmospheric Flight Mechanics Conference, Gatlinburg, Tennessee, August 1983.

2. Mease, K. D., and N. X. Vinh, "Minimum Fuel Aeroassisted Coplanar Orbit Transfer Using Lift Modulation." AIAA paper No. 83-2094, AIAA 10th Atmospheric Flight Mechanics Conference, Gatlinburg, Tennessee, August 1983.

3. Cruz, M. I., "Trajectory Optimization and Closed Loop Guidance of Aeroassisted Orbital Transfer." AAS paper No. 83-413, AAS/AIAA Astrodynamics Specialist Conference, Lake Placid, New York, August 1983.

4. Marec, J. P., "Optimal Space Trajectories." Elsevier Scientific Publishing Company, Amsterdam and New York, 1979.

5. Marchal, C., "Synthesis of the Analytical Results on Optimal Transfers Between Keplerian Orbits (Time-free case)." ONERA TP No. 482, 1967.

6. Vinh, N. X., and C. Marchal, "Analytical Solutions of a Class of Optimum Orbit Modifications." NASA CR-1379, 1969.

7. Longuski, J. M., and N. X. Vinh, "Analytic Theory of Orbit Contraction and Ballistic Entry into Planetary Atmospheres." JPL publication No. 80-58, 1980.

8. Vinh, N. X., J. R. Johannesen, J. M. Longuski, and J. M. Hanson, "Second Order Analytic Solution for Aerocapture and Ballistic Fly-Through Trajectories." AAS paper No. 83-415, AAS/AIAA Astrodynamics Specialist Conference, Lake Placid, New York, August 1983.

9. Marchal, C., "Optimization de la Phase Extra-Atmosphérique de la Montée en Orbite." La Recherche Aérospatiale, No. 116, pp. 3-12, 1967.